Available online at www.sciencedirect.com
SCIENCE DIRECT®

Catalysis Today 105 (2005) 469–478

CATALYSIS TODAY

www.elsevier.com/locate/cattod

Hydrogen production from propane in Rh-impregnated metallic microchannel reactors and alumina foams

Ingrid Aartun [a], Bozena Silberova [a,1], Hilde Venvik [a,*],
Peter Pfeifer [b], Oliver Görke [b], Klaus Schubert [b], Anders Holmen [a]

[a] *Department of Chemical Engineering, Norwegian University of Science and Technology (NTNU), Sem Sælands vei 4, NO-7491 Trondheim, Norway*
[b] *Forschungszentrum Karlsruhe GmbH, Institute for Micro Process Engineering, Postfach 3640, DE-76021 Karlsruhe, Germany*

Abstract

Rh-impregnated alumina foams and metallic microchannel reactors have been studied for production of hydrogen-rich syngas through short contact time catalytic partial oxidation (POX) and oxidative steam reforming (OSR) of propane. Effects of temperature and residence time have been compared for the two catalytic systems. Temperature profiles obtained along the central axis were valuable in understanding the different behaviour of the reactor systems. Gas phase ignition occurs in front of the metallic monolith at furnace temperatures above 700 °C, leading to lower hydrogen selectivity. Lowering the residence time below 10 ms for the microchannel monolith increases the syngas selectivity. This probably due to quenching of the gas phase reactions at high linear gas velocity, and suggests that microchannel reactors have potential for isolating kinetic effects and minimising gas phase contributions. The Rh/Al_2O_3 foam systems show higher initial syngas selectivity than the Rh-impregnated microchannel reactors, but deactivate rapidly upon temperature cycling, especially when steam is added as a reactant.

Keywords: Rh-impregnated metallic microchannel reactors; Partial oxidation; Oxidative steam reforming; Hydrogen production

1. Introduction

The short contact time reactors have been considered as promising systems for production of synthesis gas or hydrogen via fast reactions, i.e. oxidation reactions. They hold the promise of substantially increasing the throughput and thereby reducing the reactor volume. This is important in systems of a smaller scale than conventional hydrogen or syngas plants, for which steam reforming technology is well optimised, and particularly if restrictions on weight and/or volume are tight. Examples of such systems range from off-shore syngas or hydrogen plants for conversion or use of stranded natural gas, to hydrogen fuelling stations, on-board reformers for vehicles and fuel cell based combined heat and power units.

The most studied short contact time systems are probably the ceramic monoliths and foams. They have over the last years received much attention as possible syngas/hydrogen generation systems [1–8]. They have also been studied for a number of other reactions such as dehydrogenation [9–15], Fischer–Tropsch synthesis [16,17], etc. The main use of monolithic reactors, however, is as car exhaust catalysts. They are characterised by high mechanic and thermal stability using a wide variety of (mixed) ceramic materials and low-pressure drops even with very high linear gas velocities. Ceramic monoliths do not conduct heat very well, resulting in radial as well as axial temperature gradients and sometimes instabilities and local hot-spots. Ceramic monoliths and foams have differences with respect to

---

* Corresponding author. Tel.: +47 73592831; fax: +47 73594080.
E-mail address: hilde.venvik@chemeng.ntnu.no (H. Venvik).

[1] Present address: Delft University of Technology, Reactor and Catalysis Egineering, Julianalaan 136, NL-2628 BL Delft, The Netherlands.

0920-5861/$ – see front matter © 2005 Elsevier B.V. All rights reserved.
doi:10.1016/j.cattod.2005.06.025

geometry that give important differences in the flow pattern, and foams are preferred over monoliths when dealing with mass transport limited or highly exothermic reactions [18,19].

Microstructured reactors and systems have been pioneered over the last 10–15 years. By decreasing the dimensions of the flow channels and the reaction volumes to the micrometer range, new or enhanced properties can be obtained, such as extremely rapid heat exchange and mixing of reactants, highly controllable flow patterns, narrow residence time distributions and finally also well-defined catalyst geometries. Microstructured reactors often provide built-in safety because large volumes are avoided. Explosions, flames and radical reactions are locally quenched [20–22]. This, together with the opportunity for precise control of temperature, residence time and reactant dosing may facilitate processes that are dangerous or uncontrollable in conventional reactors. Enhanced selectivity to desired products and the transition from batch to continuous syntheses may be obtained for many processes. A parallelisation of chemical reactions has also been proposed to enable the standardised production of multiple cheap and small reaction devices, analogous to the development in the microelectronic industries. Microstructured reaction devices can be fabricated from a wide range of materials (metals, glass, ceramics, semiconductors), and by a wide variety of processes [22–24]. One may span a range from micro-electro-mechanical systems (MEMS)-based methods for silicon and related materials to more classical precision machining for metals. Over the last years, many research groups have investigated the possibility to use microstructured systems for syngas or hydrogen production [25–33]. The external mass transfer has been shown to strongly influence reaction rates and thereby product selectivity during fast oxidation reactions [34,35]. In partial oxidation (POX) over a Pt gauze catalyst, the mass transfer was improved by reducing the boundary layer thickness through increasing the linear gas velocity [36]. However, the small dimensions of microchannel reactors minimize the influence of the boundary layer mass transfer limitation [26].

The purpose of the present contribution is to compare the properties of metallic microchannel monoliths to those of porous alumina foams during short contact time catalytic partial oxidation and oxidative steam reforming (OSR) of propane. Both reactor systems have potential for compact processes for production of hydrogen or syngas. Oxidation reactions are extremely fast and well suited for millisecond contact time catalysis. The reaction mechanisms and the interplay between heterogeneous and homogeneous reactions for catalytic POX have been widely debated for a long time [5,37–42]. Deciding the detailed mechanisms has not been the main objective of this contribution. It has been discussed, however, whether microchannel reactors can offer new aspects to mechanistic studies.

Based on thermodynamics, the addition of steam as a reactant should facilitate higher hydrogen selectivity through water–gas shift (WGS) and steam reforming. However, as the contact time becomes shorter, mainly the kinetics will determine to which extent added steam will influence the product selectivity. In this work, the reactions with and without steam addition have been studied over a structured catalyst, and it has therefore been chosen to refer to the former case as OSR and not autothermal reforming (ATR). ATR is commonly used about the sequential industrial process where homogeneous combustion is followed by a fixed catalyst bed for equilibration of the gas [43], and in strict terms also refers to a system of no external heat supply to the reactor.

The structured supports have both been impregnated with Rh and the focus has been on how the differences in geometry and material properties between the microchannel monolith and the alumina foam influence the reactor temperatures, the selectivity to desired products, formation of by-products, and finally the catalyst stability. Rh is known to give better selectivity to hydrogen than, e.g. Pt, Pd and Ni in short contact time POX and OSR [5,44–46]. Careful temperature measurement and reporting is highly important for the interpretation of experimental data from exothermic, high temperature reactions. While the (irreversible) conversion of propane and oxygen depends strongly on the maximum temperature in the system, the product gas composition is determined by the thermodynamic equilibrium at the catalyst exit temperature given sufficient residence time. To be able to compare data between the microchannel reactor and the alumina foams, a microchannel reactor containing a larger channel along the middle axis was fabricated. Temperature profiles could therefore be obtained during reaction experiments for both systems, an approach not widely applied in reporting results on microchannel reactors.

2. Experimental

Annular pieces of alumina foam of 84% porosity (Goodfellow) were impregnated with aqueous $Rh(NO_3)$ solutions of different concentrations to obtain samples with 0.1 and 1 mg Rh, (corresponding to 0.01 and 0.1 wt.%) as calculated by solution uptake. ICP-AES analyses conducted for samples prepared in parallel to the ones used for experiments indicated obtained loadings to be higher, 0.25 and 1.7 mg Rh (0.025 wt.% and 0.17 wt.%), respectively. The foams were dried at 100 °C for 1 h, calcined in flowing air at 600 °C for 4 h and reduced in situ at 700 °C for 1 h in flowing H_2 prior to the experiments [8]. Since the Rh-impregnated foams undergo deactivation and restructuring during use [47,48], fresh samples were prepared for each set of either POX or OSR experiments.

The metallic microchannel monoliths were manufactured at the Institute for Micro Process Engineering (IMVT) at Forschungszentrum Karlsruhe from Fecralloy (72.6% Fe, 22% Cr, 4.8% Al) [49]. Two microchannel monoliths of

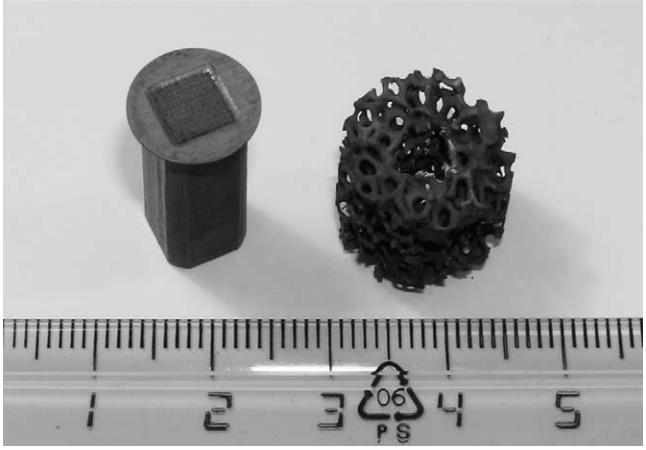

Fig. 1. Photograph of Rh-impregnated microchannel reactor and alumina foam.

identical outer dimensions were applied. Monolith 1 was a regular monolithic structure, whereas monolith 2 was equipped with a larger channel along the central axis to allow for temperature measurements inside the reactor. The monoliths were oxidized in air at 1000 °C to form a thin alumina surface layer, a procedure found to increase the total surface area by a factor of ~10 as determined by Kr-BET [28]. The microchannel monoliths were subsequently impregnated with Rh by passing an aqueous solution of $RhCl_3$ through the channels followed by drying at 120 °C overnight. The mass increase resulting from impregnation corresponds to 1 and 0.9 mg Rh for monolith 1 and 2, respectively. The Rh/Al_2O_3/Fecralloy monoliths were reduced in situ at 800 °C for 3 h in 10% H_2 in N_2 [28]. Deactivation of the Rh-impregnated monoliths was not observed after repeated experiments [50], so additional pretreatment before each experiment was not considered necessary. The two catalyst systems are shown in Fig. 1 and the relevant physical data are given in Table 1.

The same experimental set-up was applied in all reaction experiments, and has been described in more detail elsewhere [8,28]. Both catalyst systems were contained in quartz reactors and inserted in a gold insulated furnace that allows visual inspection at elevated temperatures. The Rh/Al_2O_3 foam was placed between two cordierite pieces (15 mm o.d., 4 mm i.d., 7 mm length). The 1 mm K-type thermocouples used for temperature measurements were placed inside thin quartz tubes to eliminate contributions from the small catalytic activity of the thermocouples themselves. A single tube/thermocouple was used for the foams, extending through the hole in the middle, whereas two thermocouples had to be used for monolith 1, one directly in front and one directly after the monolith. For monolith 2, the thermocouple in front was replaced with a 0.5 mm N-type thermocouple (without the quartz tube) to allow for measurements inside the 600 μm channel. A sketch showing the geometry of the two quartz reactors with critical dimensions is given in Fig. 2. The estimated heated reactor dead volumes in front of the catalysts are also given in Table 1.

The experiments were carried out using a continuous reactant flow at near-to atmospheric pressure and furnace temperatures from 300 to 950 °C. The concentration of propane was kept the same for both POX and OSR. The reactant mixture consisted of propane, oxygen and nitrogen for POX, with a C/O ratio equal to 0.8 and O/N as for air. In case of OSR, steam was added to the feed and the C/O and H_2O/O_2 ratios were 0.5 and 2.0, respectively, with N_2 to balance. The C/O and H_2O/O_2 ratios were chosen as an optimum for POX and OSR according to reported values and previous experience [8,9,28]. A total flow rate of 1000 N ml/min (0 °C, 1 atm) was chosen as reference. To examine residence time effects, a flow range of 1000–2000 N ml/min was used for the foams, whereas a slightly wider flow range, 400–2000 N ml/min was chosen for the microchannel monoliths to obtain near overlap between the residence time regimes. Water was removed from the product stream by condensation and dry samples were analyzed by gas chromatography (Agilent G2891A MicroGC). The water content in the product stream was estimated from the H- and O-balances, using N_2 as an internal standard to calculate the total volumetric flow after reaction.

The hydrogen selectivity was calculated according the equation (1):

$$S(H_2) = \frac{F_{\text{tot, out}}}{F_{\text{tot, in}}} \times \frac{C_{H_2,\text{out}}}{4\,C_{C_3H_8,\text{in}}\,X_{C_3H_8}} \qquad (1)$$

where $F_{\text{tot, in}}$ and $F_{\text{tot, out}}$ are total volumetric gas flows (N ml/min) at reactor inlet and outlet, respectively, $C_{H_2,\text{out}}$is

Table 1
Physical data of the different catalyst systems

Catalyst system	Microchannel monolith 1	Microchannel monolith 2	Alumina foams
Material	Fecralloy	Fecralloy	Alumina
$H \times W \times L$ (mm^3)/D, L (mm)	5.5 × 5.6 × 20	5.5 × 5.6 × 20	15, 12.7
No. of channels	676	572	–
Channel dimension (μm^2)	120 × 130	100 × 120	–
Geom. surface (cm^2)	67.5	50.8	200
Thermocouple channel dimension	–	600 μm × 600 μm	∅ 4 mm
Void volume (cm^3)	0.211	0.144	1.81
Rhodium loading (mg)	~1	~ 0.9	~0.25 and ~1.7
Estimated heated dead volume in front (cm^3)	4.3	4.3	6.3

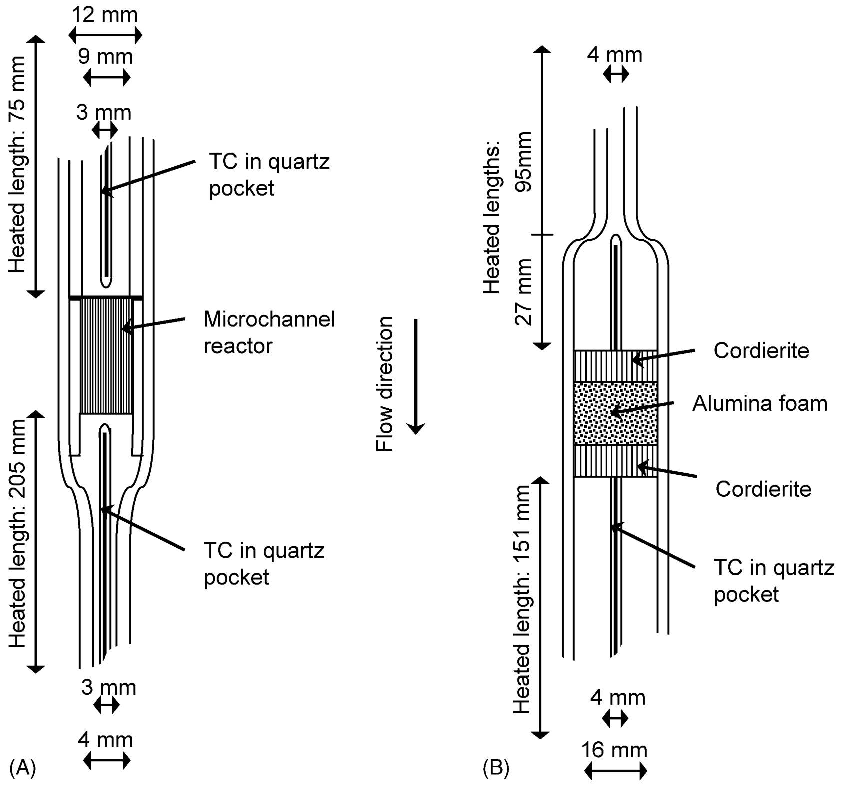

Fig. 2. Schematic drawing of the two quartz reactors loaded with (A) microchannel monolith and (B) alumina foam between two cordierite monoliths.

the concentration of hydrogen in the outlet gas, $C_{C_3H_8,\mathrm{in}}$ is the concentration of propane in the feed gas and $X_{C_3H_8}$ is the conversion of propane. The hydrogen selectivity formulated according to Eq. (1) expresses how much hydrogen is formed relative to propane converted, irrespective of steam content in the reaction mixture. The residence time was calculated as the ratio of void volume (Table 1) inside the foams or the microchannel reactors to $F_{\mathrm{tot,\ in}}$ [8,28].

3. Results and discussion

The aim of the present work has been to compare microchannel monoliths with alumina foams having similar total Rh loading and which have been subjected to comparable reaction conditions in terms of flow rate, reactant composition and furnace temperatures. The alumina foam Rh loading was measured to 0.25 and 1.7 mg, which is higher than the nominal, 0.1 and 1.0 mg, respectively. All loadings are within the same order of magnitude, and which of these are most comparable to the 1 or 0.9 mg Rh microchannel reactor loading, is influenced by particle size and structure as resulting from the preparation procedure, as well as interaction with the support. In the following, the 0.9 and 1.0 mg Rh/Al_2O_3/Fecralloy monoliths were compared to 1.7 mg Rh/Al_2O_3 foams or both loadings, except when considering the residence time effect, for which only data for 0.25 mg Rh/Al_2O_3 foams were obtained.

3.1. Temperature profiles

Temperature profiles along the reactor central axis are given in Fig. 3. The total reactant flow is 1000 N ml/min for the 1.7 mg Rh/Al_2O_3 foam and 614 N ml/min for the 0.9 mg Rh/Al_2O_3/Fecralloy monolith 2 (to ensure a residence time of 12.7 ms for monolith 2, the same as for monolith 1 at 1000 N ml/min). Catalytic ignition occurs during heating of the Rh-impregnated foams from 400 to 450 °C for both POX and OSR, and the catalyst temperature immediately exceeds 750 °C for POX and 700 °C for OSR. For the microchannel monolith, ignition is also facilitated between 400 and 500 °C, but is accompanied by a much smaller temperature rise of around 50 °C. This can be explained by the higher heat conductivity of the Rh/Al_2O_3/Fecralloy system and possibly also lower catalytic activity compared to the Rh/Al_2O_3 foam.

For the Rh-impregnated foams, the highest temperatures are observed exactly at the point where the reactant mixture enters the impregnated foams (position 0 in Fig. 3) for both POX and OSR. This is the place where the exothermic oxidation reactions mainly take place over the whole range of furnace temperatures. The microchannel monolith displays both smaller axial temperature gradients and lower differences between maximum catalyst temperature and furnace temperature than the foams for all furnace temperatures. This, in addition to the sharp difference between catalyst temperature and gas temperature indicate

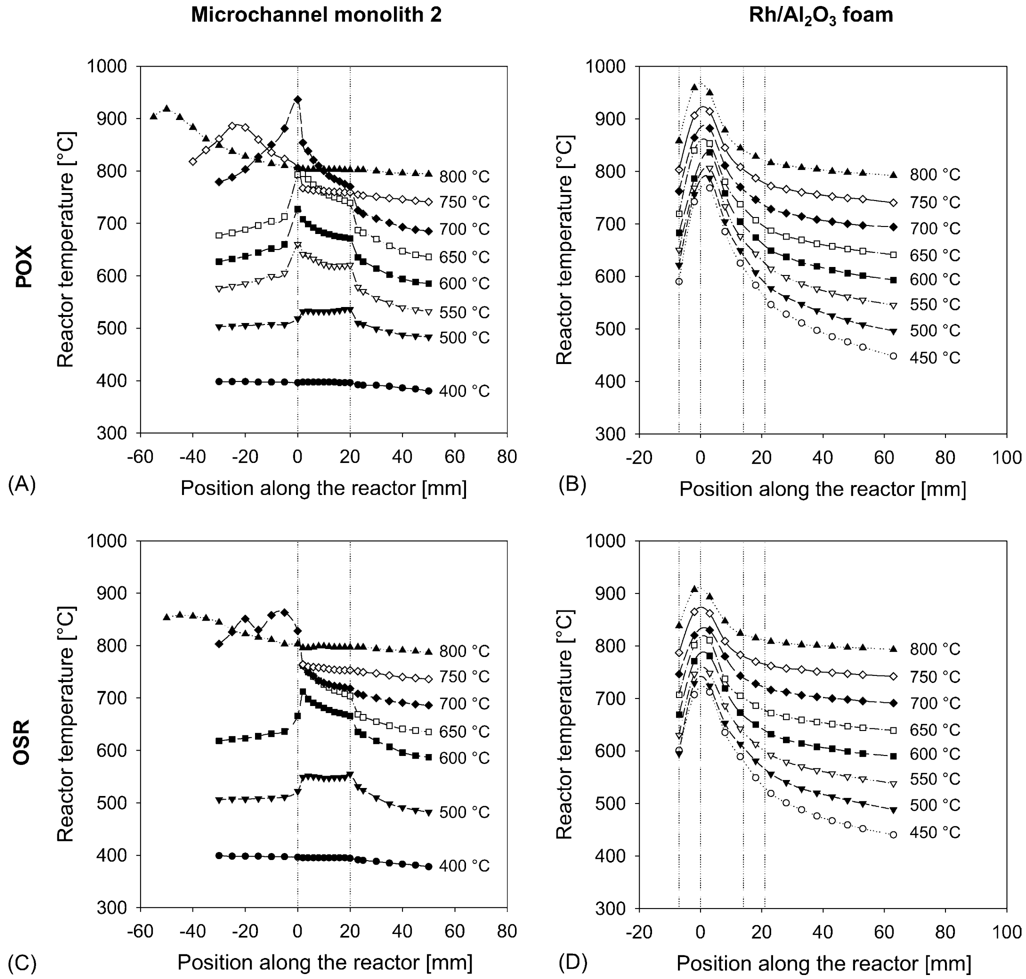

Fig. 3. Temperature profiles along the 0.9 mg Rh/Al_2O_3/Fecralloy microchannel monolith 2 (A and C) and the 1.7 mg Rh/Al_2O_3 foams (B and D) for both POX (A and B) and OSR (C and D). The vertical lines indicate the start and end of the monolith and the cordierite and foam pieces.

higher heat conductivity of the Fecralloy systems and little or no backmixing. When the furnace temperature is increased to 700 °C, the gas phase in front of the microchannel reactor ignites. At the highest furnace temperature (800 °C), the maximum temperature appears well in front of reactor (40–60 mm), and the flame could also be observed visually. After gas phase ignition, the temperature inside the microchannel reactor is almost identical to the furnace temperature. The bulk of the oxygen is converted in homogenous oxidation reactions in the gas phase, and the residence time will influence to which extent WGS and steam reforming reactions proceed on the downstream catalyst; a reaction scheme similar to conventional ATR. Even though it seems that the cordierite monolith in front of the foams to some extent prevents the ignition of the gas phase, gas phase ignition can be observed for the lowest loading (0.25 g Rh) where the temperature maxima are generally higher than for the loading used here. This and other effects of loading, together with characterisation of the as-prepared and used foams, have been reported elsewhere [8,47,48].

3.2. Temperature effects

The conversion of reactants and the selectivity to main products during POX as well as OSR are reported in Fig. 4 as a function of the furnace temperature for both the 1.0 mg Rh/Al_2O_3/Fecralloy microchannel monolith 1 and the 1.7 mg Rh/Al_2O_3 alumina foams. The total reactant flow is 1000 N ml/min, and freshly prepared Rh/Al_2O_3 foams were employed for both POX and OSR. Data from microchannel monolith 2 were not used in this figure because the flow pattern and occurrence of gas phase reactions inside the larger thermocouple channel, as well as the small catalytic activity of the thermocouple itself, slightly influence the product distribution. The product gas temperature (measured 3 mm after catalyst exit) is somewhat higher for monolith 1 than for monolith 2; a result of the higher feed gas flow. However, the deviations are small enough to conclude that Fig. 3 gives an indication of the temperature along the catalyst for a given furnace temperature.

For the 1.7 mg Rh/Al_2O_3 foams, propane conversion becomes almost complete at 800 °C furnace temperature for

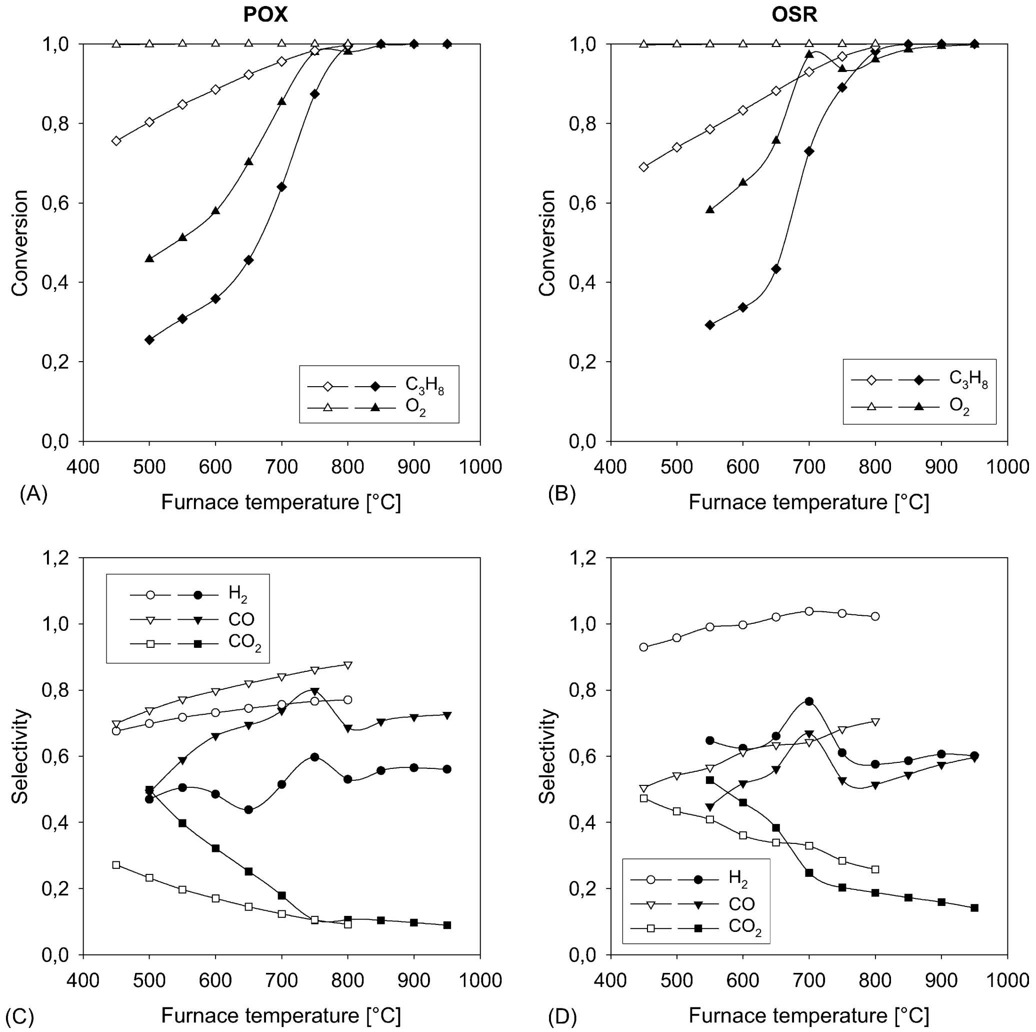

Fig. 4. Conversion (A and B) and selectivity to main products (C and D) during partial oxidation (A and C) and oxidative steam reforming (B and D) as a function of furnace temperature. The total feed gas flow is 1000 N ml/min in all experiments. Filled symbols represent the 1.0 mg Rh/Al_2O_3/Fecralloy microchannel monolith 1, open symbols the 1.7 mg Rh/Al_2O_3 foams.

both POX (99.7%) and for OSR (99.3%). The oxygen conversion is practically complete (>99.8%) from 450 °C for POX as well as OSR. Traces of oxygen (<0.05%) are detected up to 550 °C for POX and over the whole temperature range for OSR. During both POX and OSR, the hydrogen and CO selectivity increases while the CO_2 selectivity decreases with temperature. At high temperature, CO and CO_2 approach equilibrium values, while H_2 lies well below [48].

When adding steam, the hydrogen and CO_2 selectivity is shifted to higher and the CO selectivity is shifted to lower values. The increase in CO_2 and decrease in CO are practically equimolar, while the increase in hydrogen formation is slightly higher at the highest temperatures. The WGS reaction thus accounts for the major part of the increased hydrogen yield, with reforming reactions contributing as the temperature increases. The lower propane conversion for OSR can be ascribed to the lower maximum catalyst temperatures as compared to POX and the fact that less oxygen is fed compared to propane.

For the 1.0 mg Rh/Al_2O_3/Fecralloy microchannel monolith, the conversion of propane and oxygen is increasing over the temperature range 500–800 °C, but maintains substantially lower than in the foams during both POX and OSR until almost complete conversion is reached around 800 °C. This can partly be explained by the lower catalyst maximum temperatures (see Fig. 3). The residence time may also play a role, since it is almost ten times shorter than for the foams as calculated on basis of the void volume for the same total flow of reactants. Complete conversion of propane is reached at 850 °C and 900 °C furnace temperature for POX and OSR, respectively. While complete conversion of oxygen is reached for POX at 900 °C product gas/furnace temperature, trace amounts of oxygen are detected also at 950 °C for OSR.

The microchannel monolith shows higher selectivity to the total oxidation products and lower syngas selectivity over the whole temperature range. In contrast to the foams, there is no steady increase in syngas selectivity over the

Table 2
By-product selectivities (%) for Fecralloy microreactors with 1.0 mg Rh and alumina with 0.25 and 1.7 mg Rh

Component	600 °C						800 °C					
	POX			OSR			POX			OSR		
	Micro	Foam 0.025%	Foam 0.17%	Micro	Foam 0.025%	Foam 0.17%	Micro	Foam 0.025%	Foam 0.17%	Micro	Foam 0.025%	Foam 0.17%
Methane	0.9	3.9	2.4	1.7	3.6	2.4	11.2	7.5	2.4	15.5	5.9	2.8
Ethane	–	0.2	0.2	–	0.2	0.1	–	0.2	0.1	0.8	0.2	0.2
Ethene	–	1.1	0.3	–	0.7	0.1	4.6	3.7	0.4	11.2	1.8	0.5
Ethyne	–	–	–	–	–	–	4.0	8.4	–	0.5	0.1	–
Propene	0.7	0.6	0.4	0.5	0.8	0.2	0.5	0.1	0.1	1.3	0.2	0.2
Sum C_{4+}	<0.1%	–	–	–	<0.1%	–	0.5	0.6	–	0.5	<0.1%	–

Feed gas flow of 1000 N ml/min in all experiments.

furnace temperature range applied. Instead, a sharp decrease is observed between 750 and 800 °C for POX and between 700 and 750 °C for OSR. As seen from the temperature profiles obtained for corresponding experiments using monolith 2 (Fig. 3), the maximum temperature is located in front of the reactor at these product gas temperatures and above. Thus, the onset of gas phase reactions in front of the catalyst substantially reduces the selectivity to the desired products. The changes in hydrogen, CO and CO_2 formation upon addition of steam (OSR) are smaller than for the foams, but also in agreement with the WGS reaction being the main effect as long as the gas phase in front of the reactor has not ignited. After ignition, the main effect of replacing POX with OSR conditions is increased hydrocarbon by-product formation (Table 2) and reduced formation of CO with only a small increase in the formation of hydrogen.

3.3. By-product formation

Hydrocarbon by-products include methane, ethane, ethene, ethyne, propene and trace amounts of C_{4+} compounds. These are observed in various amounts depending on temperature, loading, residence time and catalyst/reactor configuration. Table 2 shows comparisons on hydrocarbon by-product formation between the 1.0 mg Rh/Al_2O_3/Fecralloy microchannel monolith 1 and both 1.7 mg Rh/Al_2O_3 and 0.25 mg Rh/Al_2O_3 foams during POX and OSR for both 600 and 800 °C furnace temperature, i.e. before and after onset of gas phase ignition of the microchannel monolith and the foam of low Rh loading.

At 600 °C furnace temperature, i.e. before gas phase ignition, the only by-products formed when using the microchannel monolith are small amounts of methane and propene. Fig. 3A and C then indicate that the maximum temperature in the system is about 720 °C, and the by-product formation can be ascribed to methanisation and dehydrogenation reactions. At the same furnace temperature (600 °C), methane is formed in much higher amounts using the foams, and together with significant amounts of ethene. The maximum temperature is measured to be 850 and 780 °C for POX and OSR, respectively (Fig. 3). The methane and ethene formation increases with decreasing Rh foam loading, which also corresponds to increased temperature [48]. Thus, the exothermic reactions proceeding at the foam entrance are supplying heat to gas-phase cracking reactions within the catalyst and adjacent cordierite. The maximum temperatures during OSR are lower than for corresponding POX experiments, but the addition of steam appears to compensate this with respect to the cracking reactions. In addition, there is some propane dehydrogenation occurring also over the foams at 600 °C furnace temperature.

The concentration of methane and ethene in the product matrix is higher for the microchannel monolith than for the foams at 800 °C furnace temperature, i.e. when the gas phase in front of the monolith has ignited, even if the maximum temperature is lower. As mentioned, the gas phase also ignites in front of the catalyst for the 0.25 mg Rh/Al_2O_3 foams at this furnace temperature. It thus appears that gas-phase reactions away from the catalyst lead to more by-product formation than when there is a closer interplay between homogeneous and heterogeneous reactions such as for the Rh/Al_2O_3 foams. Propane dehydrogenation contributes in similar amounts at 800 °C as at 600 °C furnace temperature.

Ethane is only detected in small amounts for the foams, and only after gas phase ignition for the microchannel monolith, but no clear tendencies can be extracted. Ethyne increases with temperature and is more abundant after POX. The highest ethyne selectivity is observed for the alumina foams with the lowest Rh loading, for which the maximum temperature is highest and gas phase ignition occurs (not shown here) [48]. This is in agreement with ethyne formation being solely homogeneous and increasing with temperature. C_{4+} formation is very small and follows no clear trend.

In previous work, corresponding experiments over unimpregnated alumina foams [8] and microchannel Fecralloy monoliths [28] have been reported. Whereas the formation of syngas is substantially lower, but rapidly increasing to comparable levels as the temperature reaches 1000 °C, the formation of C_1–C_4 by-products is similar when no Rh is present. Summarizing all results, we conclude that the hydrocarbon by-products are mainly formed

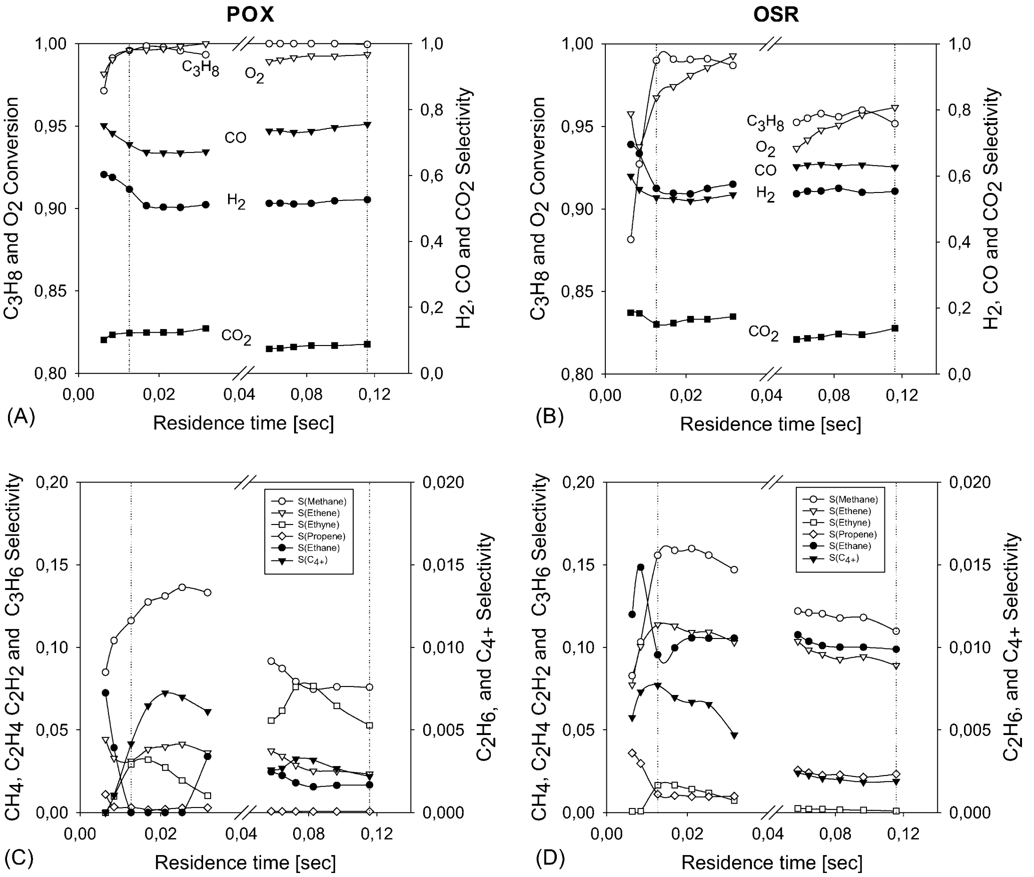

Fig. 5. Conversion and selectivity to main products (A and B) and by-products (C and D) as a function of residence time during partial oxidation (A and C) and oxidative steam reforming (B and D). The left hand series of each diagram represents experiments over the 1.0 mg Rh/Al_2O_3/Fecralloy microchannel monolith 1 for 400–2000 N ml/min total reactant flow and 800 °C furnace temperature. The right hand series of each diagram represents experiments over 0.25 mg Rh/Al_2O_3 foams for 1000–2000 N ml/min total reactant flow and 700 °C furnace temperature. The vertical lines indicate total reactant flows of 1000 N ml/min.

homogeneously. It could be that these reactions are suppressed inside the narrow microchannels also at increased temperatures. The syngas selectivity could thus be enhanced by avoiding gas phase ignition in front of the metallic monolith through minimizing dead volumes and/or applying a heat shield.

3.4. Residence time effects

Fig. 5 shows the changes in product selectivity as a function of residence time for 1.0 mg Rh/Al_2O_3/Fecralloy and 0.25 mg Rh/Al_2O_3 foams during both POX and OSR. The changes in the flow rate were made in overlapping ranges as described in the experimental section. A furnace temperature of 800 °C for the microchannel monolith and 700 °C for the alumina foams was selected to compare product selectivity when complete or nearly complete conversion of propane is reached in both catalyst systems for a total flow of 1000 N ml/min.

The hydrocarbon by-product selectivity remains relatively constant with changing residence time during both POX and OSR over the alumina foams (Fig. 5C and D), but addition of steam increases the total amount of by-products. The selectivity to each hydrocarbon by-product, except ethyne and C_{4+}, increases slightly with decreasing residence time for both POX and OSR, probably as a result of less secondary reactions over the catalyst. Ethyne and C_{4+}, undergo maxima between 60 and 80 ms residence time during POX. This residence time interval corresponds to flow rates of 1400–1600 N ml/min.

For the microchannel monolith, methane, ethene, ethyne and C_{4+} selectivities seem to follow similar trends, and generally decrease when the residence time is lowered below 10 ms, while the selectivity to propene and ethane increases below 10 ms. This is an indication of suppressed gas phase reactions; the gas flow being so high that gas phase ignition is quenched. The ethyne and C_{4+} selectivity go through maxima also for the monolith during both POX and OSR at residence times between 15 and 25 ms, corresponding to flow rates of 500–1000 N ml/min. The ethyne maxima observed may reflect the residence time in the heated dead volumes in front of the catalysts.

For the microchannel monolith, there is a noticeable increase in syngas selectivity for residence times below 10 ms for both POX and OSR, accompanied by a decrease in conversion. The conversion and selectivity at 12.7 ms residence time (1000 N ml/min total reactant flow) are in good correspondence for the overlapping points in Figs. 4 and 5 and Table 2. The increased syngas selectivity at low residence times supports the conclusion that the gas phase ignition in front of the catalyst is suppressed [44,51]. The increased syngas selectivity at low residence times is furthermore in agreement with the direct formation of hydrogen and CO being part of the reaction scheme over the catalyst, as has also been reported by others [5,40–42,44]. The hydrogen yield is at it's highest at 8.4 ms for both reactions. Since the residence time is changed by increasing the total feed gas flow while holding the concentrations constant, the catalyst temperature is probably higher at low residence times due to more heat produced in the exothermic reactions. Temperature profiles obtained at different residence times could verify our conclusion on suppressed gas phase ignition and increased maximum catalyst temperatures at high flow rates.

The 0.25 mg Rh/Al_2O_3 foams used in these experiments were subjected to a sequence of experiments with start-up and shut-down in between consisting of: (1) temperature-dependent measurements of product composition and temperature profiles followed by; (2) 7-h stability tests at one fixed furnace temperature; and finally (3) residence time effects. In the temperature-dependent experiments using 1000 N ml/min total reactant flow and over freshly prepared 0.25 mg Rh/Al_2O_3 foams (not shown here) [48], the oxygen and propane conversion was virtually complete and the hydrogen selectivity was 0.67 for POX and 0.87 for OSR at 700 °C furnace temperature. In Fig. 5A, the conversion of propane is complete but trace amounts of oxygen were detected for all residence times examined over this foam. In Fig. 5B, both propane and oxygen conversion are lower than for POX, and also substantially reduced as compared to the first OSR experiment over the fresh catalyst. The hydrogen selectivity is reduced to 0.53 and 0.55, for POX and OSR, respectively, for the residence time effect experiments as a consequence of deactivation. Hydrocarbon by-product formation was also substantially lower using the freshly prepared Rh/Al_2O_3 foam. The loss of activity and selectivity could be ascribed to deactivation through sintering as determined by FE-SEM analysis of as prepared and used catalysts, and the increased concentration of steam applied in the OSR experiments was found to accelerate this Rh sintering [47].

The residence time data for the 0.25 mg Rh/Al_2O_3 foam thus have limited value but are included to show the following: Over the flow range applied, little change in the syngas selectivity is observed, whereas this is the case for the microchannel reactor. This may point to microchannel reactor having potential for isolating kinetic effects, thereby obtaining information on complex reactions. And finally, even if the 0.25 mg Rh/Al_2O_3 catalyst shows significantly higher conversion and selectivity initially, the microchannel reactor shows comparable or even better performance over the whole flow range after only a few experiments.

3.5. Stability

Finally, we summarise the results of the stability tests reported elsewhere in more detail [47,48,50]. The Rh-impregnated foams [47,48] show little or no deactivation during time-on-stream experiments over 7 h when exposed to POX reaction conditions at 700 °C furnace temperature. Corresponding tests with OSR shows a slight deactivation tendency. Furthermore, the deactivation is stronger at the lower (0.25 mg) than the higher (1.7 mg) loading [48]. However, even more pronounced deactivation is observed upon consecutive POX or OSR experiments, indicating that temperature cycling under reactant exposure has a stronger effect than steady-state conditions. Characterization of used alumina foams by FE-SEM confirmed sintering of Rh and restructuring of the support, and the foams subjected to steam as a reactant displayed the largest Rh particles [47,48]. The microchannel monolith 1 has undergone more than 70 experimental cycles in the range from room temperature to ~1000 °C, switching between POX and OSR conditions with no sign of deactivation observed [50]. The microchannel reactors were thus not subjected to similar time-on-stream experiments. The reason behind the good stability needs to be addressed by appropriate characterisation methods, which will include destruction of the reactor(s). The Rh sintering observed for the foams could also possibly be accompanied by loss of Rh from the catalyst. This is generally very difficult to detect, and can also not be excluded for the Fecralloy monoliths despite the unchanged activity [26]. Neither of the catalyst systems show signs of carbon formation under the conditions applied.

4. Conclusions

Rh-impregnated microchannel metallic monoliths and ceramic foams have been compared under partial oxidation and oxidative steam reforming reaction conditions. Temperature profiles obtained along the catalyst/reactor axis under comparable conditions show that the gradients are smaller in the Rh/Al_2O_3/Fecralloy microchannel reactors than in the Rh/Al_2O_3 foams. Gas phase ignition occurs in front of the microchannel monolith at furnace temperatures above 700 °C for both POX and OSR for a feed gas flow of 1000 N ml/min, corresponding to a residence time of 12.7 ms. Similar gas phase ignition does not occur for the Rh/Al_2O_3 foams, except for the lowest Rh loading (0.25 mg), for which the maximum temperature is highest.

The Rh/Al_2O_3 foams show higher initial activity and syngas selectivity than the Rh/Al_2O_3/Fecralloy microchannel monolith, resulting in a product composition closer to equilibrium. The gas phase ignition observed in front of the microchannel monoliths at high temperatures is followed by a substantial decrease in the selectivity to the desired products, hydrogen and CO, as well as increased hydrocarbon by-product formation. The effect of adding steam to the reactant mixture, i.e. replacing POX with OSR conditions, can mainly be accounted for by the water–gas shift reaction, as long as gas phase ignition does not occur.

Formation of most hydrocarbon by-products can be ascribed to gas phase reactions, especially the formation of methane and ethene as cracking products and the formation of ethyne at high temperature. The gas phase reactions take place within the region near the entrance of the Rh/Al_2O_3 foams. Here, the temperature is the highest, and there is interplay between heterogeneous and homogeneous reactions. In the microchannel monolith system, gas phase reactions appear to be suppressed and the by-product formation is very low until the gas phase well in front of the catalyst ignites. The by-product formation is thus highest when there is no interplay between the homogeneous and heterogeneous reactions.

Changing the residence time interval corresponding to 1000–2000 N ml/min reactant flow has little influence on conversion and selectivity over the 0.25 mg Rh/Al_2O_3 foam. Lowering the residence time below 10 ms for the 1.0 mg Rh/Al_2O_3/Fecralloy microchannel monolith increases the syngas selectivity. This is probably due to quenching of the gas phase reactions at high linear gas velocity, and suggests that direct formation of hydrogen and CO is part of the reaction scheme. Microchannel reactors thus have potential for isolating kinetic effects and minimising gas phase contributions.

The Rh/Al_2O_3 foams show significant deactivation upon a few temperature cycles under reactant exposure, strongest with steam present in the reactant mixture. No deactivation is observed for the Rh/Al_2O_3/Fecralloy microchannel monoliths, despite repeated temperature cycling under POX and OSR reactant exposure.

Acknowledgements

The Research Council of Norway and Statoil ASA through the Gas Technology Center NTNU-SINTEF are gratefully acknowledged for their financial support.

References

[1] K. Heitnes Hofstad, B. Andersson, A. Holmgren, O.A. Rokstad, A. Holmen, Stud. Surf. Sci. Catal. 107 (1997) 415.
[2] A.S. Bodke, S.S. Bharadwaj, L.D. Schmidt, J. Catal. 179 (1998) 138.
[3] L.D. Schmidt, E.J. Klein, C.A. Leclerc, J.J. Krummenacher, K.N. West, Chem. Eng. Sci. 58 (2003) 1037.
[4] B.E. Traxel, K.L. Hohn, Appl. Catal. A 244 (2003) 129.
[5] A. Beretta, P. Forzatti, Chem. Eng. J. 99 (2004) 219.
[6] D. Neumann, G. Veser, AIChE J. 51 (2005) 210.
[7] K.A. Williams, C.A. Leclerc, L.D. Schmidt, AIChE J. 51 (2005) 247.
[8] B. Silberova, H.J. Venvik, A. Holmen, Catal. Today 99 (2005) 69.
[9] M. Huff, L.D. Schmidt, J. Catal. 149 (1994) 127.
[10] M. Huff, P.M. Torniainen, L.D. Schmidt, Catal. Today 21 (1994) 113.
[11] M. Fathi, R. Lodeng, E.S. Nilsen, B. Silberova, A. Holmen, Catal. Today 64 (2001) 113.
[12] F. Donsi, R. Pirone, G. Russo, J. Catal. 209 (2002) 51.
[13] F. Donsi, R. Pirone, G. Russo, Catal. Today 91-92 (2004) 285.
[14] J.J. Krummenacher, L.D. Schmidt, J. Catal. 222 (2004) 429.
[15] B. Silberova, M. Fathi, A. Holmen, Appl. Catal. A 276 (2004) 17.
[16] A.-M. Hilmen, E. Bergene, O.A. Lindvag, D. Schanke, S. Eri, A. Holmen, Catal. Today 69 (2001) 227.
[17] R.M. de Deugd, F. Kapteijn, J.A. Moulijn, Catal. Today 79-80 (2003) 495.
[18] D.A. Hickman, M. Huff, L.D. Schmidt, Ind. Eng. Chem. Res. 32 (1993) 809.
[19] M.V. Twigg, J.T. Richardson, Chem. Eng. Res. Des. 80 (2002) 183.
[20] M.T. Janicke, H. Kestenbaum, U. Hagendorf, F. Schuth, M. Fichtner, K. Schubert, J. Catal. 191 (2000) 282.
[21] G. Veser, Chem. Eng. Sci. 56 (2001) 1265.
[22] G. Kolb, V. Hessel, Chem. Eng. J. 98 (2004) 1.
[23] H. Löwe, W. Ehrfeld, Electrochim. Acta 44 (1999) 3679.
[24] A. Gavriilidis, P. Angeli, E. Cao, K.K. Yeong, Y.S.S. Wan, Chem. Eng. Res. Des. 80 (2002) 3.
[25] P. Pfeifer, M. Fichtner, K. Schubert, M.A. Liauw, G. Emig, in: Proceedings of the third International Conference Microreaction Technology (IMRET 3), 18–21 April 1999, Frankfurt, 1999, p. 372.
[26] M. Fichtner, J. Mayer, D. Wolf, K. Schubert, Ind. Eng. Chem. Res. 40 (2001) 3475.
[27] P. Pfeifer, K. Schubert, M.A. Liauw, G. Emig, Chem. Eng. Res. Des. 81 (2003) 711.
[28] I. Aartun, T. Gjervan, H. Venvik, O. Gorke, P. Pfeifer, M. Fathi, A. Holmen, K. Schubert, Chem. Eng. J. 101 (2004) 93.
[29] C. Horny, L. Kiwi-Minsker, A. Renken, Chem. Eng. J. 101 (2004) 3.
[30] G. Kolb, R. Zapf, V. Hessel, H. Lowe, Appl. Catal. A 277 (2004) 155.
[31] Y. Men, H. Gnaser, R. Zapf, V. Hessel, C. Ziegler, G. Kolb, Appl. Catal. A 277 (2004) 83.
[32] P. Pfeifer, L. Bohn, O. Goerke, K. Haas-Santo, Proceedings of the Statuskolloquium des Programms Mikrosystemtechnik, 10–11 February 2004, Karlsruhe, 2004, p. 213.
[33] A.Y. Tonkovich, S. Perry, Y. Wang, D. Qiu, T. LaPlante, W.A. Rogers, Chem. Eng. Sci. 59 (2004) 4819.
[34] C.T. Au, H.Y. Wang, Catal. Lett. 41 (1996) 159.
[35] Y. Boucouvalas, Z. Zhaolong, X.E. Verykios, Catal. Lett. 40 (1996) 189.
[36] M. Fathi, Catalytic partial oxidation of methane to synthesis gas (thesis), NTNU, Trondheim, 2000.
[37] M. Prettre, C. Eichner, M. Perrin, T. Faraday Soc. 43 (1946) 335.
[38] D. Dissanayake, M.P. Rosynek, K.C.C. Kharas, J.H. Lunsford, J. Catal. 132 (1991) 117.
[39] R.H. Jones, A.T. Ashcroft, D. Waller, A.K. Cheetham, J.M. Thomas, Catal. Lett. 8 (1991) 169.
[40] V.R. Choudhary, A.S. Mamman, S.D. Sansare, Angew. Chem. Int. Ed. Engl. 31 (1992) 1189.
[41] K. Heitnes Hofstad, T. Sperle, O.A. Rokstad, A. Holmen, Catal. Lett. 45 (1997) 97.
[42] W.Z. Weng, M.S. Chen, Q.G. Yan, T.H. Wu, Z.S. Chao, Y.Y. Liao, H.L. Wan, Catal. Today 63 (2000) 317.
[43] J.R. Rostrup-Nielsen, Catal. Today 18 (1993) 305.
[44] S.S. Bharadwaj, L.D. Schmidt, J. Catal. 146 (1994) 11.
[45] P.M. Torniainen, X. Chu, L.D. Schmidt, J. Catal. 146 (1994) 1.
[46] S. Ayabe, H. Omoto, T. Utaka, R. Kikuchi, K. Sasaki, Y. Teraoka, K. Eguchi, Appl. Catal. A 241 (2003) 261.
[47] B. Silberova, H.J. Venvik, J. Walmsley, A. Holmen, Catal. Today 100 (2005) 457.
[48] B. Silberova, I. Aartun, H.J. Venvik, J.C. Walmsley, A. Holmen, in preparation.
[49] K. Schubert, W. Bier, J. Brandner, M. Fichtner, C. Franz, G. Linder, in: Proceedings of the Second International Conference on Microreaction Technology (IMRET 2) 8–12 March 1998, New Orleans, 1998 (paper no. 9d).
[50] I. Aartun, H.J. Venvik, P. Pfeifer, O. Görke, K. Schubert, A. Holmen, Catal. Today, in press.
[51] K. Heitnes, S. Lindberg, O.A. Rokstad, A. Holmen, Catal. Today 21 (1994) 471.